Bionic Design Inspired by Surface Texture of Cybister's Elytra

Han Cheng[1], *Guo Ce*[1*], *Xu Tao*[2]

1. Institute of Bio-inspired Structure and Surface Engineering, College of Astronautic, Nanjing University of Aeronautics and Astronautics, Nanjing 210016, P. R. China;

2. College of Mechanical and Electrical Engineering, Nanjing University of Aeronautics and Astronautics, Nanjing 210016, P. R. China

(Received 20 March 2018; revised 20 April 2018; accepted 30 May 2018)

Abstract: Super depth digital microscope was employed to observe the macro-/micro-structure of Coleoptera's elytra. The non-smooth surface textures of elytra have shown superior performance of friction reduction and lubrication. Bionic models of regular hexagonal convex texture and circular concave texture inspired by the beetle were established and verified by numerical calculations and simulations. Further tribological experiments were performed and the results show that the circle texture has the lowest coefficient, which is consistent with the numerical calculations. The research may be further applied to new bionic surface texture designs and also work as a biological template for new bionic inventions.

Key words: bionics; surface textures; simulation; tribological test

CLC number: TB17 **Document code**: A **Article ID**: 1005-1120(2018)S-0051-08

0 Introduction

It has been a long time since human started to learn from the nature. Nature has great wisdom, encouraging people to obtain inspired and put it into practical applications[1]. In the long-term adaptation process to the nature, organisms keep on improving their internal structure, such as morphological characteristics, other related functions and the formation of body surface[2].

Coleopteran beetles belong to insecta, which has the most complex kinds compared with other animals, including the dung beetles, predacious diving beetles, cockchafers and others (Fig. 1)[3]. Due to the excellent mechanical properties of the elytra, such as drag reduction performance, wear-resistance and lubrication, the surface texture of the beetle elytra has been widely applied to structural designs[4].

Using micro manufacturing methods, the surface texture technology can produce special micro shapes arranged by certain rules and sizes in morphology. Many studies have shown that these morphologies would greatly improve the tribological properties of the surface, which cannot only effectively reduce the wear of the contact surface, but also reduce the surface friction[5-6]. The pit array textures have obvious improvements in property of anti-friction compared with

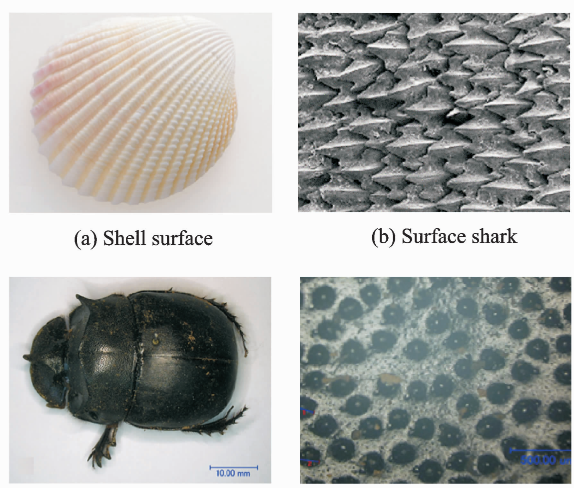

(a) Shell surface (b) Surface shark (c) Catharsius (d) Dung beetle elytra's surface

Fig. 1 Different biological surface

* Corresponding author, E-mail address: guozc@nuaa.edu.cn.

How to cite this article: Han Cheng, Guo Ce, Xu Tao, et al. Bionic design inspired by surface texture of Cybister's elytra [J]. Trans. Nanjing Univ. Aero. Astro., 2018,35(S):51-58.
http://dx.doi.org/10.16356/j.1005-1120.2018.S.051

the normal samples without surface texture processing[7]. Furthermore, pit array which had certain rules on the surface of the silicon was processed and it was concluded that the pit arrangement of high density had lower friction coefficient[8].

The previous work proved that the materials were equipped with excellent properties by reasonable surface texture design[9]. Bearing the above observation in mind, the bionic design based on the surface texture of Cybister elytra were provided. The aim of the research is to understanding in this area and the results may provide basic data for a new bionic surface texture design and also work as a biological template for new bionic inventions.

1 Materials and Methods

1.1 Animals

We take Cybister tripunctatus as the research object. The beetles used in this study were gathered from Guangzhou, Guangdong Province, China.

As shown in Fig. 2, the adult body length of this beetle is about 24—28 mm and the width is 11.5—14.3 mm. The main body of the beetle is black while the edge area of the elytra is brown. There exists a big concave on the head and obvious little concave points on the elytra.

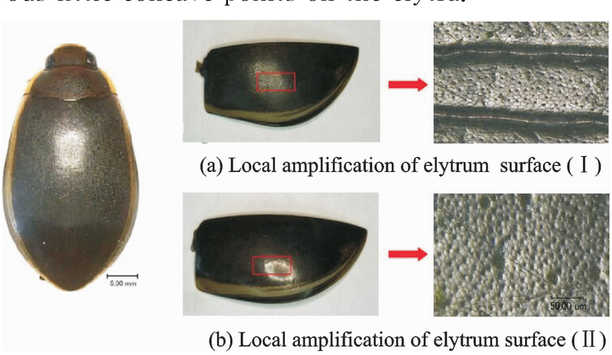

Fig. 2 One of the Cybisters taken as the specimen and Cybister elytra surface morphology

1.2 Specimen preparation and examination

In order to protect the surface structure of the beetles, some preliminary preparations were conducted before performing the observations. The beetles were placed in the beaker with ethyl acetate, and then the beaker was sealed and stored for later work. After that, the beetles were cleaned with pure water and air-dried for about 30 min, and the fridge was used to frozen death. Finally, to avoid the formation of ice on the surface of the frozen layer, the beetles were placed in the beaker filled with high concentration of alcohol and stored.

1.3 Observation on Cybister elytra's surface

Removed two pieces of Cybister elytra from alcohol solution and dried it in a ventilated place, and then placed it on the observation platform to fulfill the observation of Keyence 3-D super depth digital microscope.

2 Results and Discussion

2.1 Morphological observation

High magnification photographs of the surface structure were taken from two different beetle elytron a, b. The results showed a fairly smooth outer surface texture of elytrum b compared with elytrum a, but they both have obvious lines in certain direction. Elytron a and b are overall black in common, and only show dark yellow in the lower edge area.

Based on the local magnification photograph of elytra a, many obvious vertical grooves can be found, the measurement shows the width of grooves is 15—20 μm, and the interval between them is about 100 μm. There are a lot of micro pits on the surface of the elytra 4—6 μm in diameter and 1 μm in depth.

At the same time, a few relatively large pits in eye shape were found on the elytra 15—22 μm in diameter, in addition to that, the two elytra surfaces have closely linked polygon structure in common at the length of 5—12 μm.

2.2 Bionic surface texture design

Based on the results of microscope observation, special structures from Cybister's elytra were taken as the object of research. Two structure forms were extracted from these structures, hexagonal convex structure and circular pits structure, which established the foundation for tribological tests and theoretical models. To design the structure forms, the parameters of the circular pits in this study were selected as: The diameter was 100 μm, the depth was 5 μm and the area rate was 10.4%[10]. Moreover, the texture area ratio and height of the hexagonal shaped texture were kept in consistent with the circular shaped texture, and the side length was set as 55 μm, ensuring the hydrodynamic lubrication performance of two kinds of textures were studied under the same condition.

3 Comparison Between Surface Texture Designs

According to the mathematical model of hydrodynamic lubrication of surface texture, the performances of different bionic texture designs are compared and analyzed[11-13].

3.1 Presumed plant conditions setting

(1) The flow in the lubricant film is considered as laminar flow.

(2) The influence from volume force and inertia force on pressure is neglected.

(3) The distance between two solid surfaces is sufficient, with lubricant and without direct contact.

And the Reynolds equation can be expressed as

$$\frac{\partial}{\partial x}\left(h^3\frac{\partial p}{\partial x}\right)+\frac{\partial}{\partial y}\left(h^3\frac{\partial p}{\partial y}\right)=6\mu U\frac{\partial h}{\partial x} \tag{1}$$

where μ is the viscosity of lubricant, U the speed of upper surface, p the hydrodynamic pressure, and h the thickness of oil film.

3.2 Mathematical model of hydrodynamic lubrication

The square area of 3×3 is chosen as a computational domain, ensuring that each element has a micro texture (Fig. 3).

The radii of the circular dent unit can be expressed as

$$r_p=\frac{L}{\sqrt{\frac{\pi}{S_p}}} \tag{2}$$

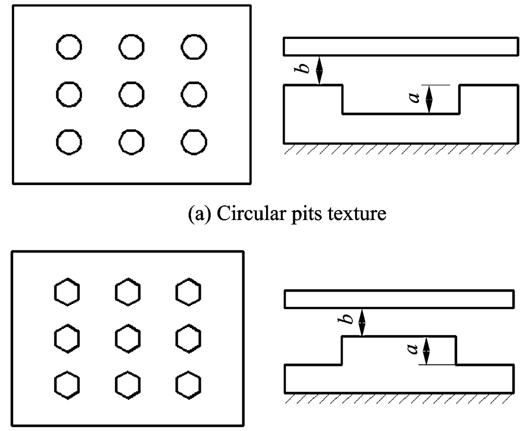

(a) Circular pits texture

(b) Hexagonal surface texture

Fig. 3 Surface texture design

And the length of the regular hexagonal convex unit is

$$l_p=\frac{L}{\sqrt{\frac{3\sqrt{3}}{2S_p}}} \tag{3}$$

The oil film thickness in the circular texture region can be expressed as

$$h(x,y)=\begin{cases}a+b & x,y\in\Delta\\ b & x,y\notin\Delta\end{cases} \tag{4}$$

And the oil film thickness in hexagonal texture region can be expressed as

$$h(x,y)=\begin{cases}b-a & x,y\in\Delta\\ b & x,y\notin\Delta\end{cases} \tag{5}$$

The finite difference method is adopted for the analysis and calculation of the Reynold equation. The pressure values at node $P_{i,j}$ can be represented by the ones of the four adjacent nodes[14]

$$AP_{i+1,j}+BP_{i-1,j}+CP_{i,j+1}+DP_{i,j-1}-EP_{i,j}=F \tag{6}$$

The calculation formula of the average dimensionless lubricant film pressure value is

$$P_{av}=\frac{\iint P(x,y)\mathrm{d}x\mathrm{d}y}{A} \tag{7}$$

The formula for calculating the average shear stress is

$$F=\frac{1}{A}\sum\sum\tau(x,y)\mathrm{d}x\mathrm{d}y \tag{8}$$

The friction coefficient is determined by $f=F/P_{av}$, the friction coefficients of the hexagonal convex texture and the circular surface texture can be expressed as

$$f=\frac{\mu U}{W}\left(\frac{S_p}{b}+\frac{1-S_p}{a+b}\right) \tag{9}$$

$$f=\frac{\mu U}{W}\left(\frac{S_p}{a+b}+\frac{1-S_p}{b}\right) \tag{10}$$

The pressure value of plane lubrication film is calculated by Matlab programming method, combined with the parameters in Ref. [15]. In this simulation, the velocity of the relative motion between the surfaces is 0.06 m/s, and the viscosity of the lubricant is 0.03 Pa • s.

3.3 Analysis of simulation results

3.3.1 The hexagonal convex texture

Fig. 4 is the non-dimensional lubrication film pressure distribution diagram of the hexagonal surface texture. The pressure distribution of the remaining textures exhibited a periodic variation law, except for the parts near the inlet and outlet place of the lubricant. At the same time, in the convergence region where the lubricant flew into the texture, the lubricant film pressure value is positive, and there exists a limit of maximum value. And the coefficient of friction is calculated as $f=4.232\times10^{-3}$.

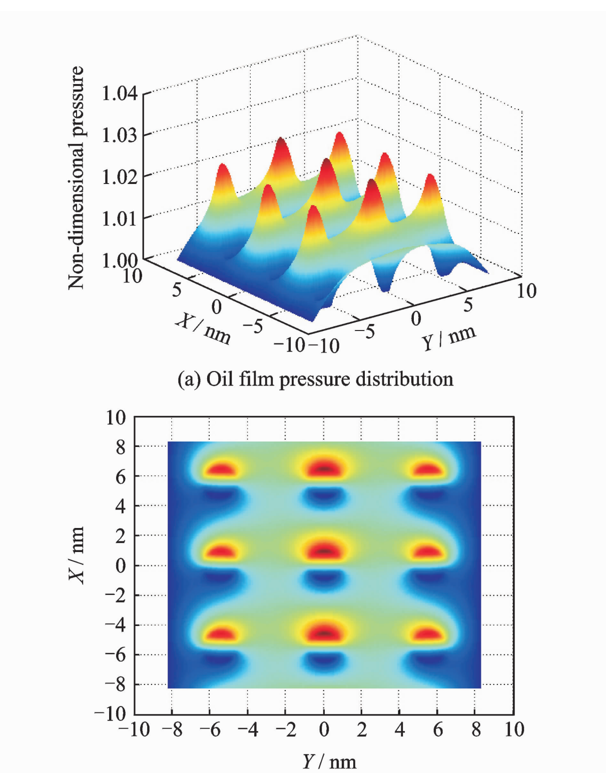

(a) Oil film pressure distribution

(b) Vertical view of the oil film pressure distribution

Fig. 4 Dimensionless oil film pressure distribution of hexagonal texture

3.3.2 The circular surface texture

Fig. 5 is the non-dimensional lubrication film pressure distribution diagram of the circular surface texture. The circular texture has the same lubrication film pressure distribution characteristics as the hexagonal one, but the maximum lubricating film pressure is less than hexagonal texture. And the coefficient of friction is calculated as $f=2.795\times10^{-3}$.

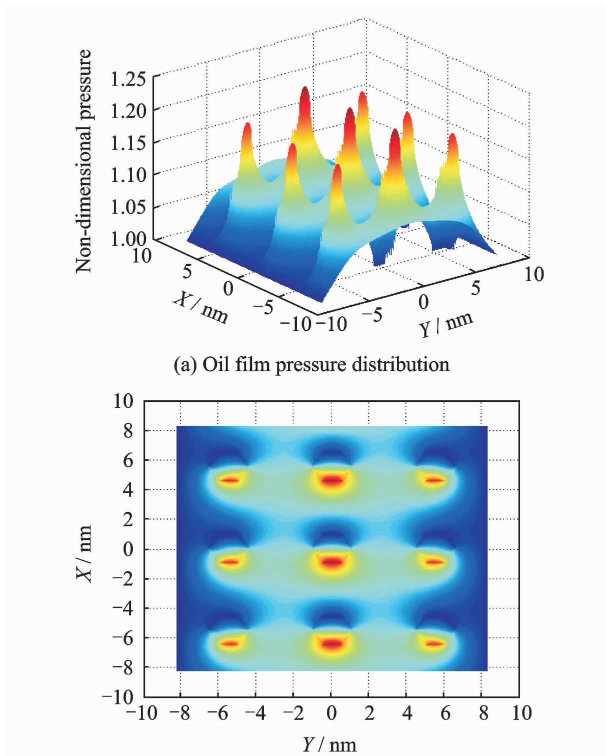

(a) Oil film pressure distribution

(b) Vertical view of oil film pressure distribution

Fig. 5 Dimensionless oil film pressure distribution of circular texture

4 Tribological Tests

By analysis results of the model, the circular texture has smaller friction coefficient, which proves that the circular texture can well reduce friction and resist wear. The relationship between different texture designs and tribological properties was investigated and analyzed through the tribological tests.

4.1 Experimental equipment

The friction wear testing machine UMT-2 is applied to the tests, and the friction coefficients are tanken as judge standard (Fig. 6).

Fig. 6 Friction wear testing machine UMT-2

4.1.1 Experimental molds

The microstructures for experimental molds were studied by SEM (Fig. 7). The diameter of circular texture is about 99.14 μm, the height is about 5.3 μm, and the area rate is 10.4%, while the diameter of hexagonal texture is about 53.68 μm, the depth is about 5.6 μm, and the area rate is 10.4%.

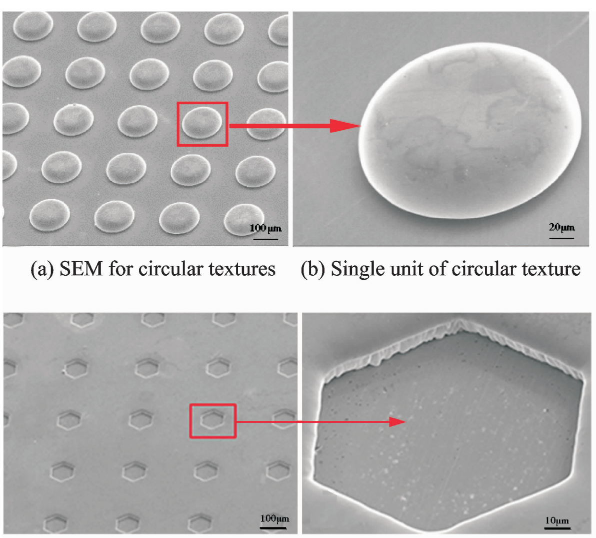

(a) SEM for circular textures (b) Single unit of circular texture

(c) SEM for hexagonal textures (d) Single unit of hexagonal texture

Fig. 7 SEM for circular and hexagonal textures

4.1.2 Materials for specimens

UHMWPE are taken to make the specimens, which have the molecular weighting up to 3×10^6. As is shown in Table 1, the diameter of the material is set as 50 mm and the thickness is about 4 mm.

Medical stainless steel SUS316 is used to make testing piece, the diameter of which is about 8 mm, after grinding and polishing, the mirror face effect is achieved (Table 2).

Table 1 Main properties of UHMWPE

Density/ (g • cm^{-3})	Hardness (HRB)	Melting point/℃	Water absorption/%
0.93	40	135	≤0.01

Table 2 Main properties of stainless steel SUS316

Yield strength/ MPa	Tensile strength/ MPa	Density/ (g • cm^{-3})
310 MPa	620 MPa	8.03

4.1.3 Reagents preparation

Lubricants is mainly made up of the powder of sodium hyaluronate, which is bought from Nanjing Doulai Biological Technology Co. Ltd. As is shown in Fig. 8.

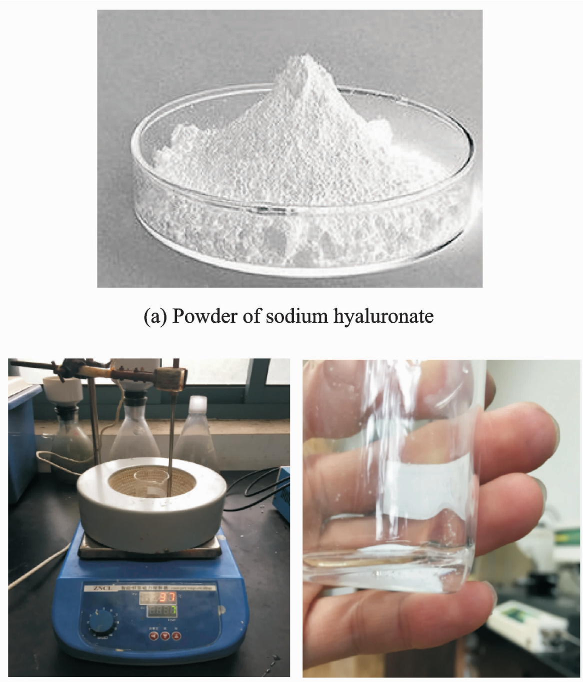

(a) Powder of sodium hyaluronate

(b) Magnetic mixer (c) Sodium hyaluronate solution

Fig. 8 Preparation of sodium hyaluronate solution

(1) Weigh the powder of sodium hyaluronate with a balance.

(2) Pour the powder into a beaker containing deionized water.

(3) Place the beaker in a magnetic mixer, set the rotation rate and the temperature to 37 ℃ for about 45 min.

4.2 Experiment contents and process

Common texture, the circular texture, and the hexagonal texture are tested by spherical tribology test, in order to obtain the best texture design (Table 3).

Table 3 Environmental conditions and parameters

Environmental condition	Specific parameter
Testing piece	SUS316 stainless steel ball
Specimens	UHMWPE
Loading/N	5
Speed/($m \cdot s^{-1}$)	0.06
Testing time/min	75
Lubricant	sodium hyaluronate solution

5 Results and Analysis

Three sets of parallel tests for common texture are carried out to obtain three different friction coefficient results (Fig. 9).

Three sets of parallel tests for circular texture are carried out to obtain three different friction coefficient results (Fig. 10).

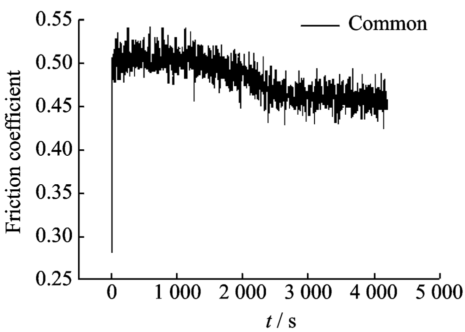

(a) Result of Test A

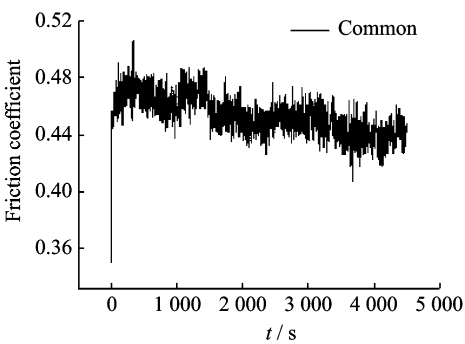

(b) Result of Test B

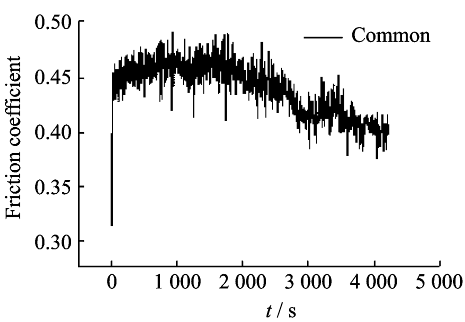

(c) Result of Test C

Fig. 9 Tests for friction coefficient of common texture

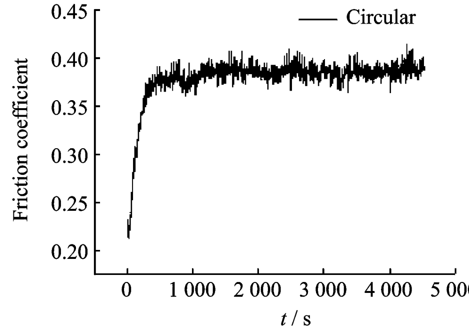

(a) Result of Test A

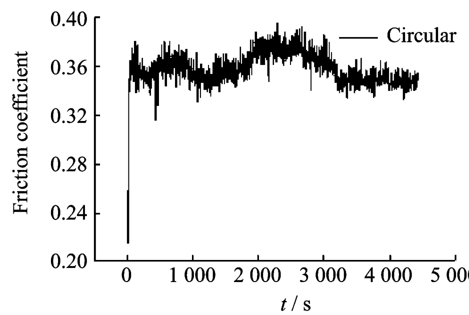

(b) Result of Test B

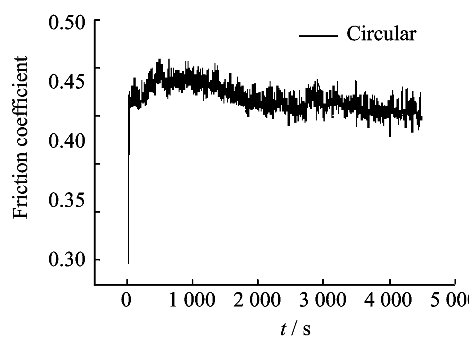

(c) Result of Test C

Fig. 10 Tests for friction coefficient of circular texture

Three sets of parallel tests for hexagonal texture are carried out to obtain three different friction coefficient results (Fig. 11).

The average values of friction coefficient for the three groups are obtained and compared (Fig. 12).

6 Conclusions

We made the morphology observation, bionic design, theoretical calculation, and experiments in order to explore the best bionic design scheme.

First, the hydrodynamic lubrication model of regular hexagonal convex texture and circular concave convex texture were established to study the texture of the friction and wear-resistance properties. Then numerical methods based on the

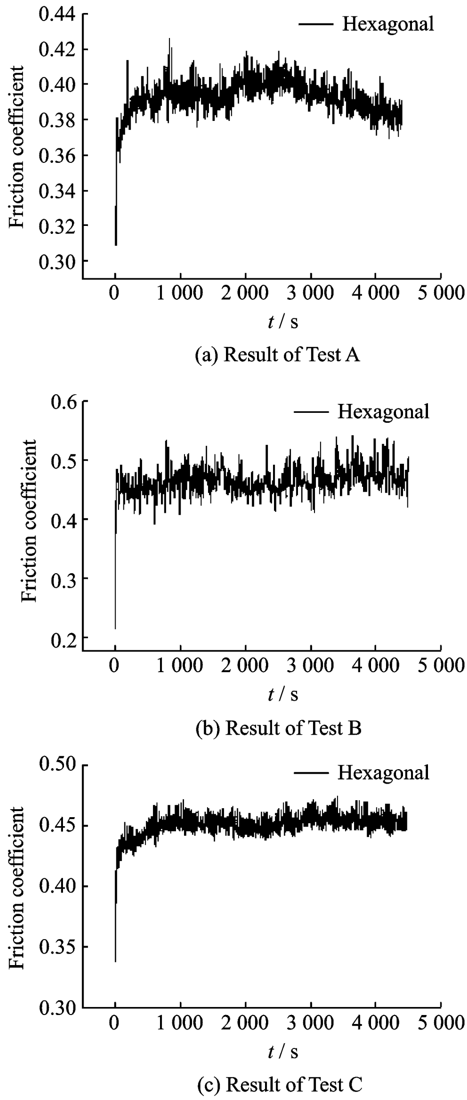

Fig. 11 Tests for friction coefficient of hexagonal texture

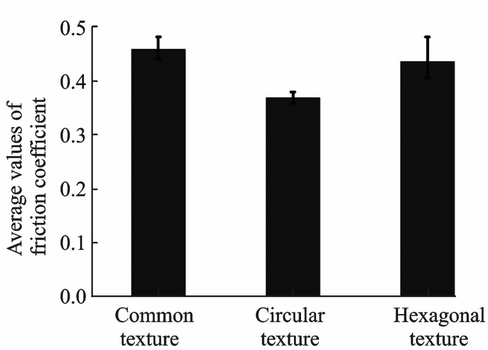

Fig. 12 Average friction coefficient of each specimen

Reynolds equation were used to calculate the pressure of the lubricating film through Matlab programming calculation. And the distribution of oil film pressure and thickness were obtained, respectively, and the friction coefficients of two kinds of texture surfaces were calculated. Finally, experiments on spherical tribology are carried out, the results show that the circular texture has the smallest friction coefficient, followed by the hexagonal texture, and the friction coefficient of the common texture is the biggest. By comparing the coefficient of friction, which was taken as the standard for evaluating the friction-wearing and lubrication properties of the textures, the circular pit texture was finally chosen as the optimal design scheme.

The results in this study may provide inspiration for a new bionic surface texture design and also work as a biological template for new bionic inventions.

Acknowledgements

This work was supported in part by the National Natural Science Foundation of China (Nos. 51175249, 51475230).

References:

[1] GAO F J, LIU X L. Comments on the question of characteristic scale in the study on spatial structures and bionic engineering[J]. Spatial Structures, 2001, 7(1):44-50.

[2] YE J M. Social bionic theory[M]. Hong Kong: Chunghwa Book, 1992.

[3] REN L Q, YANG Z J, HAN Z W. Non-smooth wearable surfaces of living creatures and their bionic application[J]. Transactions of the Chinese Society for Agricultural Machinery, 2005, 36(7):144-147.

[4] LU Yongxiang. The significance and development of bionics[J]. Scientific Chinese, 2004(4): 22-24. (in Chinese)

[5] CAO Xuping, LUO Qingsheng, WANG Fei, et al. Research and producing on an assembly and animation of a kind of bionic flying robot[J]. Modern Computer, 2007 (1):76-80. (in Chinese)

[6] QIAO Rui. Study on thermal and mechanical properties of lightweight structure inspired by beetle elytra [D]. Nanjing:Nanjing University of Aeronautics and Astronautics, 2013. (in Chinese)

[7] YANG Zhixian. The micro structure of beetle elytra, bionic research on mechanical properties and bonding mechanism [D]. Nanjing: Nanjing University of Aeronautics and Astronautics, 2008. (in Chinese)

[8] CHENG H, LI J Q. Structure of the integumentary surface of the dung beetle copris ochus motschulsky

and its relation to non-adherence of substrate particles [J]. Acta Entomologica Sinica, 2002, 45(2): 175-181.

[9] WANG G L, REN L Q, CHEN B C. The fractal characteristics of non-smooth structure unit distribution Catharsius surface geometry[J]. Transactions of the Chinese Society of Agricultural Machinery, 1997, 28(4):5-9.

[10] LI J Q, ZHU H. Surface texture and its influence on tribological properties[J]. Lubrication Engineering, 2009(2):94-97.

[11] CONG Q, WANG L C, CHU R F. Research of bionic convex shape reducing adhesion and resistance of soil plate push[J]. Construction Machinery and Equipment, 1995, 11:14-16.

[12] HILLS B A. Boundary lubrication in vivo[J]. Journal of Engineering in Medicine, 2000, 214(1):83-94.

[13] WANG X, KATO K, ADACHI K, et al. The effect of laser texturing of SiC surface on the critical load for the transition of water lubrication mode from hydrodynamic to mixed[J]. Tribology International, 2001, 34:703-711.

[14] WANG X, KATO K, ADACHI K, et al. Loads carrying capacity map for the surface texturedesign of SiC thrust bearing sliding in water[J]. Tribology International, 2003, 36:187-197.

[15] PETTERSSON U, JACOBSON S. Textured surfaces for improved lubrication at high pressure and low sliding speed of roller/piston in hydraulic motors [J]. Tribology International, 2007, 40(2):355-359.

Mr. **Han Cheng** received the B. S. degree in Communication Engineering and M. S. degree in Mechanical Design and Theory from Nanjing University of Aeronautics and Astronautics, Nanjing, China, in 2015 and 2018, respectively.

Prof. **Guo Ce** received the B. S. and Ph. D. degrees in Mechanical Engineering from Jiangnan University, Wuxi, China, in 1993 and Southeast University, Nanjing, China, in 2003, respectively. From 2007 to 2008, she was a postdoctoral research fellow in Newcastle University, Newcastle, UK. From 2013 to present, she has been with the College of Astronautics, Nanjing University of Aeronautics and Astronautics (NUAA), where she is currently a full professor of the Institute of Bio-inspired Structure and Surface Engineering. Her research has focused on biomimetic multi-functional structure and materials, and animal motion bionics, etc.

Mr. **Xu Tao** received the B. S. degree in Nanjing Forest University and M. S. degree in Nanjing University of Aeronautics and Astronautics, China, in 2013 and 2016, respectively. In August 2016, he joined Xuzhou Heavy Machinery Co., Ltd., as a construction engineer. In October 2017, he joined the branch office of Shenzhen Mindray Bio-Medical Electronics Co., Ltd..

(Production Editor: Xu Chengting)